ELSEVIER

Journal of Organometallic Chemistry 579 (1999) 235–242

Journal of Organo metallic Chemistry

Ditelluroether complexes of Group 6 metal carbonyls: synthesis, spectroscopic studies and a comparison with dithio- and diseleno-ether analogues

Andrew J. Barton, William Levason *, Gillian Reid

Department of Chemistry, University of Southampton, Southampton SO17 1BJ, UK

Received 9 November 1998

Abstract

The syntheses of [M(CO)$_4$(L–L)] (M = Cr, Mo or W, L–L = MeTe(CH$_2$)$_3$TeMe, PhTe(CH$_2$)$_3$TePh or *o*-C$_6$H$_4$(TeMe)$_2$) are described along with some dithioether (L–L–MeS(CH$_2$)$_2$SMe, MeS(CH$_2$)$_3$SMe) and diselenoether (L–L = MeSe(CH$_2$)$_2$SeMe, MeSe(CH$_2$)$_3$SeMe or *o*-C$_6$H$_4$(SeMe)$_2$) analogues. The complexes have been characterised by IR, ^{1}H-, ^{13}C{^{1}H}-, ^{77}Se{^{1}H}-, ^{125}Te{^{1}H}- and ^{95}Mo-NMR spectroscopy, FAB mass spectrometry and analysis. The structure of [Cr(CO)$_4${MeSe(CH$_2$)$_2$SeMe}] is reported. Comparison of the spectroscopic data reveals that ditelluroethers are significantly better σ-donors towards low valent metal centres than their lighter analogues. © 1999 Elsevier Science S.A. All rights reserved.

Keywords: Chromium; Molybdenum; Tungsten; Ditelluroether; Dithioether; Diselenoether

1. Introduction

Substituted Group 6 carbonyls have been studied in great detail with a wide variety of ligand types [1], and are thus very suitable systems in which to explore the properties of new ligands. Ditelluroether ligands have been available for about 10 years [2] and their complexes with Group 8–11 metals in positive oxidation states have been examined in some detail [3–6]. In contrast, their chemistry with low valent metal and organometallic species remains largely unexplored. We have undertaken the synthesis and study of complexes of various metal carbonyls with these ligands in parallel with studies of thio- or seleno- analogues, to place the trends within Group 16 in context. Complexes with manganese and rhenium carbonyl halides have been described [7], and we report here complexes of type [M(CO)$_4$(L–L)] (M = Cr, Mo or W; L–L = ditelluroether). The corresponding dithioether and diselenoether complexes have received considerable attention [8–17]. We have prepared a range of known and new complexes for comparison purposes since we required vibrational data recorded under the same conditions for all the complexes, and literature multinuclear NMR data are very limited.

2. Results

2.1. Ditelluroether complexes

The syntheses of the complexes of the three ditelluroethers (MeTe(CH$_2$)$_3$TeMe, PhTe(CH$_2$)$_3$TePh, *o*-C$_6$H$_4$(TeMe)$_2$) and a range of dithioether and diselenoether analogues (Table 1) were straightforward, utilising reaction of the ligand with [Cr(CO)$_4$(nbd)] (nbd = norbornadiene (bicyclo-[2,2,1]-hepta-2,5-diene)), [Mo(CO)$_4$(nbd)] or [W(CO)$_4${Me$_2$N(CH$_2$)$_3$NMe$_2$}] in toluene, followed by recrystallisation from CHCl$_3$ and

---

* Corresponding author. Fax: +44-1703-593-781.

E-mail address: wxl@soton.ac.uk (W. Levason)

PII: S0022-328X(99)00005-4

Table 1
IR spectroscopic data

Complex	ν(CO) cm^{-1}[a]
$[Cr(CO)_4\{MeTe(CH_2)_3TeMe\}]$	2000(m), 1887(s,br), 1858(s)
$[Mo(CO)_4\{MeTe(CH_2)_3TeMe\}]$	2015(m), 1908(s,br), 1862(s)
$[W(CO)_4\{MeTe(CH_2)_3TeMe\}]$	2010(m), 1894(s,br), 1859(s)
$[Cr(CO)_4\{PhTe(CH_2)_3TePh\}]$	2003(m), 1903(sh), 1891(s,br), 1870(s)
$[Mo(CO)_4\{PhTe(CH_2)_3TePh\}]$	2018(m), 1907(s,br), 1875(s)
$[W(CO)_4\{PhTe(CH_2)_3TePh\}]$	2013(m), 1895(s,br), 1869(s)
$[Cr(CO)_4\{o\text{-}C_6H_4(TeMe)_2\}]$	2005(m), 1902(s,br), 1873(s)
$[Mo(CO)_4\{o\text{-}C_6H_4(TeMe)_2\}]$	2020(m), 1920(sh), 1911(s), 1880(s)
$[W(CO)_4\{o\text{-}C_6H_4(TeMe)_2\}]$	2015(m), 1900(s,br), 1875(s)
$[Cr(CO)_4\{MeS(CH_2)_2SMe\}]$	2016(s), 1898(s,br), 1860(s)
$[Mo(CO)_4\{MeSCH_2)_2SMe\}]$	2024(s), 1910(s,br), 1863(s)
$[W(CO)_4\{MeS(CH_2)_2SMe\}]$	2019(m), 1897(s,br), 1859(s)
$[Mo(CO)_4\{o\text{-}C_6H_4(SMe)_2\}]$	2028(m), 1917(s,br), 1870(s)
$[Cr(CO)_4\{MeS(CH_2)_3SMe\}]$	2015(s), 1900(s), 1890(sh), 1854(s)
$[Mo(CO)_4\{MeS(CH_2)_3SMe\}]$	2023(s), 1910(s,br), 1895(sh), 1856(s)
$[W(CO)_4\{MeS(CH_2)_3SMe\}]$	2018(m), 1897(s), 1890(sh), 1852(s)
$[Cr(CO)_4\{MeSe(CH_2)_2SeMe\}]$	2011(s), 1900(sh), 1889(s), 1860(s)
$[Mo(CO)_4\{MeSe(CH_2)_2SeMe\}]$	2021(m), 1909(s,br), 1862(s)
$[W(CO)_4\{MeSe(CH_2)_2SeMe\}]$	2016(m), 1895(s,br), 1858(s)
$[Cr(CO)_4\{MeSe(CH_2)_3SeMe\}]$	2009(m), 1894(s,br), 1852(s)
$[Mo(CO)_4\{MeSe(CH_2)_3SeMe\}]$	2020(m), 1908(s), 1895(sh), 1855(s)
$[W(CO)_4\{MeSe(CH_2)_3SeMe\}]$	2015(m), 1896(s), 1885(sh), 1850(s)
$[Cr(CO)_4\{o\text{-}C_6H_4(SeMe)_2\}]$	2015(s),1902(s,br), 1866(s)
$[Mo(CO)_4\{o\text{-}C_6H_4(SeMe)_2\}]$	2025(m),1914(s,br), 1870(m)
$[W(CO)_4\{o\text{-}C_6H_4(SeMe)_2\}]$	2019(m), 1901(s,br), 1866(s)

[a] In CH_2Cl_2 solution, m, medium; s, strong; br, broad.

pentane. The complexes are air-stable in the solid state and reasonably so in solution when pure. They were insoluble in hydrocarbons, but very soluble in chlorocarbon solvents. The formulation of the new complexes as *cis*-tetracarbonyls $[M(CO)_4(L–L)]$ follows from the analyses, the FAB mass spectra, and their IR spectra (Table 1). The FAB mass spectra (Section 4) show for each complex a parent ion and often fragments corresponding to sequential carbonyl loss. The IR spectra in CH_2Cl_2 solution in most cases show only three ν(CO) bands. Theory for a *trans* isomer predicts one IR active mode (E_u) and for a *cis*, four stretches ($2A_1 + B_1 + B_2$). The observation of only three bands in the majority of cases is due to the failure to resolve the A_1 and B_1 modes at ca. 1900 cm^{-1}. A similar effect has been noted in some dithioether complexes [15].

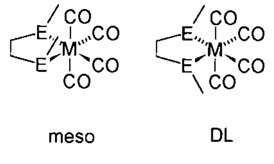

Scheme 1. *Meso* and *DL* invertomers of $[M(CO)_4$(ditelluroether)].

For a $[M(CO)_4$(ditelluroether)] complex two stereoisomers (invertomers) are expected (*meso* and *DL*, Scheme 1), which interconvert by pyramidal inversion at tellurium. When inversion is slow on the NMR timescale, the two invertomers are readily distinguished in the ^1H-NMR spectra. Previous studies [18] have established that for dithioether and diselenoether complexes, the energy barriers to inversion are dependent on several factors, viz.: the donor Se > S; the ligand backbone $–(CH_2)_2– > –(CH_2)_3– > o\text{-}C_6H_4$; and the metal W > Cr > Mo. The only quantitative data on ditelluroethers is from $[PtMe_3I$(ditelluroether)] complexes [6], which revealed that inversion was a higher energy process in these complexes than in the diselenoether analogues. It is clear from Table 2 that the present complexes conform to the expected patterns. Thus, all the ditelluroether complexes show resonances for both invertomers in the ^1H-NMR spectra at 300 K (at 300 MHz) consistent with relatively high inversion barriers.

The observed $^{13}C\{^1H\}$-NMR spectra (Table 2) also depend upon whether the complex is undergoing fast inversion or not, this time on the energy of the ^{13}C-NMR scale. If fast inversion is occuring then only two δ(CO) resonances are expected due to the CO groups mutually *trans* and those *trans*$_{L–L}$. However, if inversion is slow, five δ(CO) resonances are expected by symmetry, two due to CO *trans*$_{L–L}$ in the *meso* and *DL* invertomers, respectively, one due to the mutually *trans* CO in the *DL* form, and two due to the CO$_{transCO}$ in the *meso* form, which are distinguished by being *syn* or *anti* to the R-groups on the ligands. In practice (Table 2), whilst five resonances are seen in some cases, e.g. $[Cr(CO)_4\{MeTe(CH_2)_3TeMe\}]$, in others, e.g. $[Cr(CO)_4\{o\text{-}C_6H_4(TeMe)_2\}]$, only four are seen, which is due to accidental coincidence of the δ(CO) *trans*$_{L–L}$ in the two invertomers.

The $^{125}Te\{^1H\}$-NMR data on the complexes are given in Table 3. In all cases, coordination to the $M(CO)_4$ fragment produces characteristic frequency shifts, the magnitude of the coordination shifts (Δ) reflecting the chelate ring size present, those in 5-membered rings being markedly greater than those in 6-membered ones [2]. For a particular ligand, the largest high-frequency shift is observed in the chromium complex, a smaller shift occurs for the molybdenum analogue, and the smallest for the tungsten. In the cases of $[W(CO)_4\{RTe(CH_2)_3TeR\}]$ (R = Me or Ph), the δ(Te) resonance is to low frequency of that of the free ligand.

The relative population of *meso* and *DL* invertomers also varies with the metal and ligand combination. For $o\text{-}C_6H_4(TeMe)_2$ complexes of Cr or Mo in CH_2Cl_2 solution, the two invertomers have similar abundances, but the for the tungsten complex the *meso:DL* ratio is ca. 10:7. In the complexes of $MeTe(CH_2)_3TeMe$, the

Table 2
^{1}H- and ^{13}C{^{1}H}-NMR data

Complex	$\delta(^{1}H)^{a}$	$\delta(^{13}C\{^{1}H\})^{b}$
$[Cr(CO)_4\{MeTe(CH_2)_3TeMe\}]$	1.70(m)(CH_2) 2.12, 2.18(Me), 2.68(m)(CH_2Te)	228.1, 227.9, 224.0, 223.2, 221.5(CO), 25.8, 25.6(CH_2), 6.3, 5.9(CH_2Te), −10.5, −12.5(Me)
$[Mo(CO)_4\{MeTe(CH_2)_3TeMe\}]$	1.93(m)(CH_2), 2.16, 2.21(Me), 2.68(m)(CH_2Te)	215.7, 211.5, 211.0, 209.3(CO), 27.2(CH_2), 7.6, 6.5(CH_2Te), −10.4, −11.4(Me)
$[W(CO)_4\{MeTe(CH_2)_3TeMe\}]$	1.90(m)(CH_2), 2.23, 2.28(Me), 2.73(m)(CH_2Te)	206.2(170), 204.8(−), 203.9(−), 201.9(120)(CO)^{c}, 28.1, 27.8(CH_2), 8.7, 7.6(CH_2Te), −8.0, −9.5(Me)
$[Cr(CO)_4\{PhTe(CH_2)_3TePh\}]$	1.71(m)(CH_2), 2.83(m), 3.0(m)(CH_2Te), 7.3–7.8(m)(Ph)	227.7, 227.3, 224.4, 222.0, 220.5(CO), 137–129 (Ph), 27.0, 26.3(CH_2), 11.8, 11.6(CH_2Te)
$[Mo(CO)_4\{PhTe(CH_2)_3TePh\}]$	1.9(m)(CH_2), 2.85(m), 2.95(m)(CH_2Te), 7.3–7.8(m)(Ph)	215.6, 211.2, 210.8, 208.6(CO), 137–130 (Ph), 28.0, 27.4(CH_2), 13.3, 12.8(sh), (CH_2Te)
$[W(CO)_4\{PhTe(CH_2)_3TePh\}]$	1.9(m)(CH_2), 2.9(m), 3.1(m) (CH_2Te), 7.4–7.8(m)(Ph)	205.5(–), 205.3(160), 205.0(–), 203.5(125), 203.4(–), 137–129(Ph), 28.9, 27.9(CH_2), 13.9, 13.5(CH_2Te)
$[Cr(CO)_4\{o\text{-}C_6H_4(TeMe)_2\}]$	2.31, 2.41(Me), 7.4(m), 7.8(m)(C_6H_4)	230.7, 221.6, 220.9, 220.5(CO) 139–126(C_6H_4), −4.0, −4.6(Me)
$[Mo(CO)_4\{o\text{-}C_6H_4(TeMe)_2\}]$	2.33, 2.42(Me), 7.4(m), 8.0(m)(C_6H_4)	218.3, 208.8, 208.6, 208.4(CO), 139–123 (C_6H_4), −3.5, −3.8(Me)
$[W(CO)_4\{o\text{-}C_6H_4(TeMe)_2\}]$	2.43, 2.53(Me), 7.4(m), 8.0(m)(C_6H_4)	208.7(–), 208.6(–), 201.6(–), 201.1(–), 200.5(–)(CO), 139–123(C_6H_4), −1.5, −1.7(Me)
$[Cr(CO)_4\{MeS(CH_2)_2SMe\}]$	2.35(Me), 2.65(CH_2)	227.1, 216.3(CO), 35.4(CH_2), 24.6(Me)
$[Mo(CO)_4\{MeS(CH_2)_2SMe\}]$	2.44(Me), 2.74(CH_2)	217.5, 206.5(CO), 35.2(CH_2), 25.3(Me)
$[W(CO)_4\{MeS(CH_2)_2SMe\}]$	2.62(Me), 2.78(CH_2)	207.9(164), 201.4(135)(CO), 36.5(CH_2), 26.8(Me)
$[Mo(CO)_4\{o\text{-}C_6H_4(SMe)_2\}]$	2.83(Me), 7.4(m), 7.8(m)(C_6H_4)	217.6, 205.8 (CO), 138–130(C_6H_4), 32.6(Me)
$[Cr(CO)_4\{MeS(CH_2)_3SMe\}]$	2.14(m)(CH_2), 2.41(Me), 2.78(m)(CH_2S)	225.8, 217.0 (CO), 38.6(CH_2S), 25.5(Me), 24.5(CH_2)
$[Mo(CO)_4\{MeS(CH_2)_3SMe\}]$	2.20(m)(CH_2), 2.49(Me), 2.88(m)(CH_2S)	217.0, 207.1(CO), 39.7(CH_2S), 26.5(Me), 25.0(CH_2)
$[W(CO)_4\{MeS(CH_2)_3SMe\}]$	2.32(m)(CH_2), 2.67(Me), 3.02(m)(CH_2S)	207.6(156), 202.7(126) (CO), 39.9(CH_2S), 28.0(Me), 24.9(CH_2)
$[Cr(CO)_4\{MeSe(CH_2)_2SeMe\}]$	2.14, 2.23(Me), 3.1, 3.3(CH_2)	229.0, 219.2, 217.8, 216.7(CO), 28.5, 28.0(CH_2), 14.5, 13.5(Me)
$[Mo(CO)_4\{MeSe(CH_2)_2SeMe\}]$	2.2(v,br,Me), 3.0(v,br,CH_2)	217.9, 207.9, 207.4, 207.0(CO), 31.1, 26.9(CH_2), 14.9(sh), 14.2(Me)
$[W(CO)_4\{MeSe(CH_2)_2SeMe\}]$	2.37, 2.55(Me), 3.3, 3.35(CH_2)	208.3(sh), 208.2(156), 203.2(–), 202.1(–), 200.8(–)(CO), 29.4, 28.0(CH_2), 16.8, 15.6(Me)
$[Cr(CO)_4\{o\text{-}C_6H_4(SeMe)_2\}]$	2.60(br,Me), 7.4(m), 7.8(m)(C_6H_4)	227.8, 211.6(CO), 134–126 (C_6H_4), 20.1(Me)
$[Mo(CO)_4\{o\text{-}C_6H_4(SeMe)_2\}]$	2.66(Me), 7.4(m), 7.9(m)(C_6H_4)	218.0, 206.7(CO), 135–130(C_6H_4), 22.9(Me)
$[W(CO)_4\{o\text{-}C_6H_4(SeMe)_2\}]$	2.43, 2.53(Me), 7.4(m), 7.9(m)(C_6H_4)	208.4(165), ~201(v,br)(–), 135–130(C_6H_4), 24.8(Me)
$[Cr(CO)_4\{MeSe(CH_2)_3SeMe\}]$	2.18(CH_2), 2.30(Me), 2.8(br,CH_2Se)	227.0, 219.0(CO), 29.1(CH_2Se), 25.5(CH_2), 14.3(Me)
$[Mo(CO)_4\{MeSe(CH_2)_3SeMe\}]$	2.25(CH_2), 2.37(Me), 2.8(br,CH_2Se)	216.8, 208.3(CO), 30.5(CH_2Se), 26.3(CH_2), 15.5(Me)
$[W(CO)_4\{MeSe(CH_2)_3SeMe\}]$	2.39(br,CH_2), 2.53(Me), 3.0(br,CH_2Se)	~206(v,br), ~203(v,br)(CO), 30.0(CH_2Se), 26.0(CH_2), 16.4(Me)

[a] In $CDCl_3$ all resonances are singlets unless otherwise indicated.

[b] In CH_2Cl_2–10% $CDCl_3$ containing $Cr(acac)_3$.

[c] Values in parentheses are $^{1}J(^{183}W–^{13}C)$/Hz, (–) indicates couplings unclear or satellites not observed.

invertomers are of approximately equal abundance for all three metals, but in complexes of $PhTe(CH_2)_3TePh$, the *DL* invertomer predominates (> 70%), possibly indicating destabilising interactions between the Ph groups and the axial carbonyl group in the *meso* form.

2.2. Diselenoether and dithioether complexes

A range of selenium and sulfur ligand analogues (Tables 1 and 2) were examined for comparison purposes as explained above. The ^{1}H- and ^{13}C{^{1}H}-NMR data show that all the dithioether complexes are inverting rapidly on the appropriate timescales at ambient temperatures, consistent with previous detailed studies [14,16]. The behaviour of the diselenoether complexes is more complicated. Thus, the NMR spectra of $[M(CO)_4(MeSeCH_2CH_2SeMe)]$ (M = Cr or W) at 300 K show sharp resonances attributable to the *meso* and *DL* forms, whereas $[M(CO)_4\{MeSe(CH_2)_3SeMe\}]$ (M = Cr or Mo) and $[Mo(CO)_4\{o\text{-}C_4H_4(SeMe)_2\}]$ exhibit much simpler 'averaged' spectra due to rapid inversion. The other four complexes (Table 2) show broadened resonances typical of systems near to coalescence. These results conform with the expected trends in inversion barriers [18] outlined above. ^{77}Se-NMR data for the diselenoethers are given in Table 3.

Table 3
^{77}Se{^{1}H}-, ^{125}Te{^{1}H}- and ^{95}Mo-NMR data

Complex	δ(^{77}Se{^{1}H} or ^{125}Te{^{1}H})[a]	Δ[b]	δ(^{95}Mo)[c]
$[Cr(CO)_4\{MeTe(CH_2)_3TeMe\}]$	259, 253	152	–
$[Mo(CO)_4\{MeTe(CH_2)_3TeMe\}]$	169.5, 162	61	−1597(200), −1621(200)
$[W(CO)_4\{MeTe(CH_2)_3TeMe\}]$	94, 93	−10	–
$[Cr(CO)_4\{PhTe(CH_2)_3TePh\}]$	550, 548	83	–
$[Mo(CO)_4\{PhTe(CH_2)_3TePh\}]$	477, 476	10	−1580(sh), −1594(300)
$[W(CO)_4\{PhTe(CH_2)_3TePh\}]$	396, 390	−73	–
$[Cr(CO)_4\{o\text{-}C_6H_4(TeMe)_2\}]$	864, 856	488	–
$[Mo(CO)_4\{o\text{-}C_6H_4(TeMe)_2\}]$	725, 723.5	382	−1667(140)
$[W(CO)_4\{o\text{-}C_6H_4(TeMe)_2\}]$	664, 657	289	–
$[Cr(CO)_4\{MeSe(CH_2)_2SeMe\}]$	289, 236	141.5	–
$[Mo(CO)_4\{MeSe(CH_2)_2SeMe\}]$	213, 206	88.5	−1432(160)
$[W(CO)_4\{MeSe(CH_2)_2SeMe\}]$	183, 179	60	–
$[Cr(CO)_4\{o\text{-}C_6H_4(SeMe)_2\}]$	387, 384	183.5	–
$[Mo(CO)_4\{o\text{-}C_6H_4(SeMe)_2\}]$	331	129	−1437(200)
$[W(CO)_4\{o\text{-}C_6H_4(SeMe)_2\}]$	306, 303	103	–
$[Cr(CO)_4\{MeSe(CH_2)_3SeMe\}]$	98	24	–
$[Mo(CO)_4\{MeSe(CH_2)_3SeMe\}]$	64	−10	−1340(200)
$[W(CO)_4\{MeSe(CH_2)_3SeMe\}]$	37, 24[d]	−43	–
$[Mo(CO)_4\{MeS(CH_2)_2SMe\}]$	–	–	−1372(85)
$[Mo(CO)_4\{o\text{-}C_6H_4(SMe)_2\}]$	–	–	−1375(260)
$[Mo(CO)_4\{MeS(CH_2)_3SMe\}]$	–	–	−1294(50)

[a] In CH_2Cl_2–10%$CDCl_3$ relative to neat external Me_2Se or Me_2Te.

[b] $\delta_{\text{complex}} - \delta_{\text{free ligand}}$.

[c] Relative to external aqueous Na_2MoO_4 ($W_{1/2}$ in parentheses Hz).

[d] No resonance observed at 300 K, presumably due to inversion broadening, data reported obtained at 230 K.

2.3. ^{95}Mo-NMR

The $[Mo(CO)_4\{MeTe(CH_2)_3TeMe\}]$ complex exhibits two ^{95}Mo resonances consistent with the presence of both invertomers, whilst for $[Mo(CO)_4\{PhTe(CH_2)_3TePh\}]$ there is a high frequency shoulder on the major ^{95}Mo resonance. However, the ^{95}Mo-NMR spectra of the other seven complexes (Table 3), each contain only a single resonance. The δ(Mo) shifts sequentially to high frequency with donor Te < Se < S and with chelate ring size 5 < 6. For seven of the complexes, the ^{95}Mo-NMR spectra do not distinguish the invertomers, indicating either that inversion is fast on the molybdenum NMR time scale or that the individual resonances are not resolved in the line width. Since the lines are relatively sharp (≤ 300 Hz), the former seems much more likely. This behaviour is in marked contrast to $[Mn(CO)_3X(\text{ditelluroether})]$, $[PtX_2(\text{ditelluroether})]$ or $[PtMe_3X(\text{ditelluroether})]$ ($X =$ halide), where the ^{55}Mn- or ^{195}Pt-NMR spectra show well-separated resonances for the individual invertomers [3,6,7]. On cooling the samples, the lines broaden rapidly, possibly due to the ^{95}Mo quadrupole (^{95}Mo, $I = 5/2$) and low-temperature spectra were not obtained, an effect previously observed for dithioether complexes [14]. The interpretation of metal nuclei NMR chemical shifts is usually based upon the Ramsey equation, specifically upon the paramagnetic term σ_p. Deshielding results from small values of ΔE (the average excitation energy—essentially the weighted mean ligand field splitting) and with a reduced d-electron delocalisation. The shielding of the Mo nuclei with donor, Te > Se > S, could thus be due to increasing ligand field splitting as Group 16 is descended, and/or better delocalisation (π-acceptance) in the same order. Theoretical studies by Schumann and Hoffmann [19] concluded that π effects were negligible in Group 16 donor ligands, and thus, the trends in the molybdenum NMR data are most likely due to increased σ-donation in the order S → Se → Te.

2.4. Structure of $[Cr(CO)_4\{MeSe(CH_2)_2SeMe\}]$

The important bond lengths and angles are shown in Table 4 and the molecule in Fig. 1. The structure reveals the expected *cis* disubstituted distorted octahedron about Cr, with Se–Cr–Se 86.59(5)°, the C–Cr–Se angles slightly greater than 90° and the C–Cr–C less than 90°. The ligand adopts the *DL* conformation with Cr–Se 2.517(1), 2.520(2) Å, and $Cr–C_{cis\,Se}$ 1.891(8), 1.892(7) and $Cr–C_{trans\,Se}$ 1.832(7), 1.8314(8)Å. The structural data may be compared with those in $[Cr(CO)_4(DL\text{-}EtS(CH_2)_2SEt)]$ where $Cr–S = 2.418(1)$, $Cr–C_{cis\,S} = 1.887(3)$, and $Cr–C_{trans\,S} = 1.831(3)$Å [10]. The differences in the Cr-chalcogen bond length reflects the larger size of Se, and the Cr–C distances are not significantly different. Unfortunately, we have been unable to grow good quality crystals of a chromium telluroether to complete the comparisons.

Table 4
Selected bond lengths and angles for [$Cr(CO)_4(MeSeCH_2CH_2SeMe)$]

Bond lengths (Å)			
Se(1)–Cr(1)	2.517(1)	Se(1)–C(5)	1.946(7)
Se(1)–C(6)	1.956(7)	Se(2)–Cr(1)	2.520(2)
Se(2)–C(7)	1.955(7)	Se(2)–C(8)	1.948(7)
Cr(1)–C(1)	1.891(8)	Cr(1)–C(2)	1.892(7)
Cr(1)–C(3)	1.832(7)	Cr(1)–C(4)	1.834(8)
O(1)–C(1)	1.149(8)	O(2)–C(2)	1.154(8)
O(3)–C(3)	1.159(8)	O(4)–C(4)	1.172(8)
C(6)–C(7)	1.515(10)		
Bond angles (°)			
Cr(1)–Se(1)–C(5)	107.2(2)	Cr(1)–Se(1)–C(6)	102.5(2)
C(5)–Se(1)–C(6)	97.1(3)	Cr(1)–Se(2)–C(7)	103.5(2)
Cr(1)–Se(2)–C(8)	108.4(2)	C(7)–Se(2)–C(8)	97.0(3)
Se(1)–Cr(1)–Se(2)	86.59(5)	Se(1)–Cr(1)–C(1)	90.2(2)
Se(1)–Cr(1)–C(2)	91.3(2)	Se(1)–Cr(1)–C(3)	93.2(2)
Se(1)–Cr(1)–C(4)	178.9(2)	Se(2)–Cr(1)–C(1)	91.6(2)
Se(2)–Cr(1)–C(2)	92.3(2)	Se(2)–Cr(1)–C(3)	179.7(2)
Se(2)–Cr(1)–C(4)	92.4(2)	C(1)–Cr(1)–C(2)	175.9(3)
C(1)–Cr(1)–C(3)	88.5(3)	C(1)–Cr(1)–C(4)	89.6(3)
C(2)–Cr(1)–C(3)	87.6(3)	C(2)–Cr(1)–C(4)	88.9(3)
C(3)–Cr(1)–C(4)	87.9(3)		

3. Comparisons of Group 16 ligand properties.

The characterisation of ditelluroether complexes with the Group 6 carbonyls is of interest in its own right, but it also offers an opportunity to compare ligand properties of dithioethers, diselenoethers and ditelluroethers. For this purpose we used the $\nu(CO)$ stretching vibrations and the relative magnitude of the ^{77}Se- and ^{125}Te-NMR shifts. In principle, the $\delta(CO)$ shifts in the $^{13}C\{^1H\}$-NMR spectra and for the tungsten complexes the $^1J(^{13}C-^{183}W)$ coupling constants on the $CO_{trans\,L-L}$ resonances, should also provide useful information. However, due to the complications related to the pyramidal inversion processes, line-broadening in some cases or low abundance of one invertomer in others, these data are incomplete and less useful. Consideration of the data in Tables 1–3 shows that the parameters of interest are also sensitive to the metal centre present, the chelate ring size and the ligand substituents. Hence, we restrict discussion initially to the complexes [$M(CO)_4\{MeE(CH_2)_3EMe\}$] and [$M(CO)_4\{o\text{-}C_6H_4(EMe)_2\}$] (E = S, Se or Te) for each metal in turn. Consideration of $\nu(CO)$ shows that for a given M, the frequencies (especially that of the A_1 mode of the CO's trans L–L) fall with donor from S to Se and then there is a rather greater fall to Te. On the conventional M–CO bonding model, this reflects greater electron density on the metal centre resulting in greater π-backbonding to the CO's and hence a weaking of the C–O bond. The most obvious way of increasing the metal electron density is increased σ-donation from the Group 16 donors. As Group 16 is descended, the electronegativity of the donor atoms fall, and providing the match in orbital overlap and energy remains good, increasing σ-donation would be expected. In metals in positive oxidation states, especially as the formal charge rises, the contraction of the metal d-orbitals has been suggested to lead to mismatch in orbital size and energy at tellurium, but in the expanded d-orbitals of zero-valent metals as in the present case this is unlikely to be a problem.

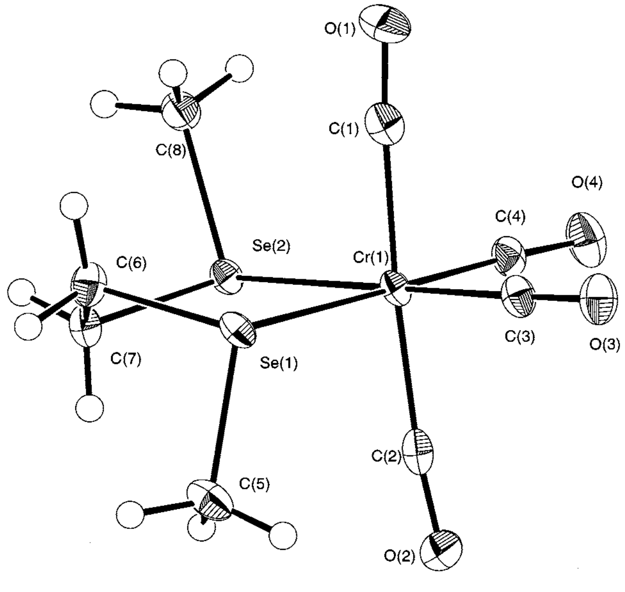

Fig. 1. Structure of [$Cr(CO)_4\{MeSe(CH_2)_2SeMe\}$] with atom numbering scheme. Ellipsoids are drawn at the 40% probability level.

Turning to the ^{77}Se and ^{125}Te chemical shifts (Table 3), as stated above (Section 2.2) the shifts are very sensitive to the ring size and the metal present. However, if we compare the data on complexes of the same metal with isostructural ligands, we see similar trends, with larger coordination shifts in the tellurium spectra as usually observed [2]. In many organoselenium and organotellurium systems the relative magnitude of the heteroatom chemical shifts ($\delta(Te)/\delta(Se)$) are ca. 1.8 [2,20], and this ratio is also found in several series of seleno- and telluroether complexes with platinum metal halides [3]. However, in the present carbonyl systems for a fixed metal and ligand type the ratios are significantly greater [$o\text{-}C_6H_4(EMe)_2$, M = Cr 2.25, M = Mo 2.2, M = W 2.2; $MeE(CH_2)_3EMe$, M = Cr 2.6, M = Mo 2.6, M = W 3.0[1]], which indicates that the tellurium centre is deshielded to an unexpected degree and is consistent with greater Te → M σ-donation. The ^{95}Mo-NMR data discussed in Section 2.3 also support the conclusion that the telluroethers are the best σ-donors in the series of ligands. The spectroscopic data clearly

---

[1] The $^{77}Se\{^1H\}$-NMR spectrum of [$W(CO)_4\{MeSe(CH_2)_3SeMe\}$] was not observed at room temperature, and the data obtained at 230 K was used (see Table 3). Since ^{77}Se-NMR shifts often vary with temperature the comparison is subject to larger errors than in the other cases, but nonetheless exhibits the expected trend.

support the proposal of Schumann and Hoffmann [19] that telluroethers are the best donors among group 16 ligands towards low valent metal centres.

4. Experimental

All preparations were performed under a dinitrogen atmosphere using standard Schlenk techniques. The complexes are air-stable as solids. The $M(CO)_6$ were obtained from Aldrich and converted into $[Cr(CO)_4(nbd)]$, $[Mo(CO)_4(nbd)]$ and $[W(CO)_4\{Me_2N(CH_2)_3NMe_2\}]$ by minor modifications of literature routes [21,22]. The tellurium ligands were made as described [23].

IR spectra were run in 1 mm solution cells fitted with NaCl optics on a Perkin Elmer 1600 FTIR spectrometer. Mass spectra (FAB) on a VG analytical 70-250-SE instrument using 3-NOBA as matrix. ^1H NMR spectra were obtained from $CDCl_3$ solutions on a Bruker AM300 operating at 300 MHz and referenced to TMS. $^{13}C\{^1H\}$-, $^{77}Se\{^1H\}$-, $^{125}Te\{^1H\}$- and ^{95}Mo-NMR spectra were obtained on a Bruker AM360 at 90.5, 68.68, 113.6 and 23.4 MHz, respectively, and referenced respectively to TMS, neat external Me_2Se, neat external Me_2Te, and aqueous $[MoO_4]^{2-}$. Samples were contained in 10 mm OD tubes containing CH_2Cl_2–10% $CDCl_3$ solutions, and for $^{13}C\{^1H\}$ studies, $Cr(acac)_3$ and a pulse delay of 2 s were used to overcome the slow relaxation of the carbonyl groups.

The complexes were prepared by the same general methods, examples of which are described.

4.1. *[Cr(CO)$_4${MeTe(CH$_2$)$_3$TeMe}]*

$[Cr(CO)_4(nbd)]$ (0.12g, 0.47 mmol) was dissolved in degassed toluene (15 cm^3) and the ligand (0.15 g, 0.47 mmol) added via a syringe. The reaction mixture was stirred at 50°C overnight and then the toluene removed in vacuo. The residue was dissolved in $CHCl_3$ (5 cm^3), filtered and cold *n*-pentane added to yield a bright yellow powder. This was filtered off, washed with *n*-pentane and vacuum dried. Yield 0.15 g 67%. (Found: C, 21.7; H, 2.2. $C_9H_{12}CrO_4Te_2$ requires C, 21.9; H, 2.4%). FAB-MS M^+ 492, 464, 436, 408, 380. Calc. for $C_9H_{12}^{52}CrO_4^{180}Te_2$; $(P)^+$ 496, $(P-CO)^+$ 468, $(P-2CO)^+$ 440, $(P-3CO)^+$ 412, $(P-4CO)^+$ 384.

4.2. *[Cr(CO)$_4${o-C$_6$H$_4$(TeMe)$_2$}]*

Yield 52% (Found: C, 27.8; H, 2.0. $C_{12}H_{10}CrO_4Te_2$ requires C, 27.4; H, 1.9%). FAB-MS M^+ 526, 440. Calc. for $C_{12}H_{10}^{52}CrO_4^{130}Te_2$; $(P)^+$ 530, $(P-3CO)^+$ 446.

4.3. *[Cr(CO)$_4${PhTe(CH$_2$)$_3$TePh}]*

Yield 73% (Found: C, 36.5; H, 2.7. $C_{19}H_{16}CrO_4Te_2$ requires C, 37.1; H, 2.6%). FAB-MS M^+ 616, 560. Calc. for $C_{19}H_{16}^{52}CrO_4^{130}Te_2$; (P^+) 620, $(P-2CO)^+$ 564.

4.4. *[Cr(CO)$_4${MeS(CH$_2$)$_2$SMe}]*

Yield 57% (Found: C, 33.7; H, 3.5. $C_8H_{10}CrO_4S_2$ requires C, 33.6; H, 3.5%). FAB-MS M^+ 286, 258, 230, 202. Calc. for $C_8H_{10}^{52}CrO_4^{32}S_2$; $(P)^+$ 286, $(P-CO)^+$ 258, $(P-2CO)^+$ 230, $(P-3CO)^+$ 202.

4.5. *[Cr(CO)$_4${MeS(CH$_2$)$_3$SMe}]*

Yield 56% (Found: C, 35.4; H, 3.9. $C_9H_{12}CrO_4S_2$ requires C, 36.0; H, 4.0%). FAB-MS M^+ 300, 272, 244, 216. Calc. for $C_9H_{12}^{52}CrO_4^{32}S_2$; $(P)^+$ 300, $(P-CO)^+$ 272, $(P-2CO)^+$ 272, $(P-3CO)^+$ 244, $(P-4CO)^+$ 216.

4.6. *[Cr(CO)$_4${MeSe(CH$_2$)$_2$SeMe}]*

Yield 50% (Found: C, 25.2; H, 2.7. $C_8H_{10}CrO_4Se_2$ requires C, 25.3; H, 2.6%). FAB-MS M^+ 382, 354, 326. Calc. for $C_8H_{10}^{52}CrO_4^{80}Se_2$; $(P)^+$ 380, $(P-CO)^+$ 352, $(P-3CO)^+$ 324.

4.7. *[Cr(CO)$_4${MeSe(CH$_2$)$_3$SeMe}]*

Yield 69% (Found: C, 27.2; H, 2.7. $C_9H_{12}CrO_4Se_2$ requires C, 27.4; H, 3.1%). FAB-MS M^+ 396, 368, 340, 312. Calc. for $C_9H_{12}^{52}CrO_4^{80}Se_2$; $(P)^+$ 396, $(P-CO)^+$ 368, $(P-2CO)^+$ 340, $(P-4CO)^+$ 312.

4.8. *[Cr(CO)$_4${o-C$_6$H$_4$(SeMe)$_2$}]*

Yield 72% (Found: C, 33.4; H, 2.5. $C_{12}H_{10}CrO_4Se_2$ requires C, 33.7; H, 2.3%). FAB-MS M^+ 430, 402, 374, 346. Calc. for $C_{12}H_{10}^{52}CrO_4^{80}Se_2$ $(P)^+$ 430, $(P-CO)^+$ 402, $(P-2CO)^+$ 374, $(P-4CO)^+$ 346.

4.9. *[Mo(CO)$_4${MeTe(CH$_2$)$_3$TeMe}]*

$[Mo(CO)_4(nbd)]$ (0.12g, 0.4 mmol) was dissolved in degassed toluene (15 cm^3) and the ligand (0.13g, 0.4 mmol) added via a syringe. The reaction mixture was stirred at room temperature overnight and then the toluene removed in vacuo. The residue was dissolved in $CHCl_3$ (5 cm^3), filtered and cold *n*-pentane added to yield a pale yellow powder. This was filtered off, washed with *n*-pentane and vacuum dried. Yield 0.15g, 69%. (Found: C, 20.4; H, 2.3. $C_9H_{12}MoO_4Te_2$ requires C, 20.2; H, 2.3%). FAB-MS M^+ 536, 508. Calc. for $C_9H_{12}^{98}MoO_4^{130}Te_2$; $(P)^+$ 542, $(P-CO)^+$ 514.

4.10. [Mo(CO)$_4${o-C$_6$H$_4$(TeMe)$_2$}]

Yield 60% (Found: C, 25.5; H, 1.8. $C_{12}H_{10}MoO_4Te_2$ requires C, 25.3; H, 1.8%).

4.11. [Mo(CO)$_4${PhTe(CH$_2$)$_3$TePh}]

Yield 74% (Found: C, 34.5; H, 2.4. $C_{19}H_{16}MoO_4Te_2$ requires C, 34.6; H, 2.4%). FAB-MS M$^+$ 660, 632, 604. Calc. for $C_{19}H_{16}^{98}MoO_4^{130}Te_2$; (P)$^+$ 666, (P − CO)$^+$ 638, (P − 2CO)$^+$ 610.

4.12. [Mo(CO)$_4${MeS(CH$_2$)$_2$SMe}]

Yield 63% (Found: C, 29.2; H, 3.1. $C_8H_{10}MoO_4S_2$ requires C, 29.1; H, 3.0%). FAB-MS M$^+$ 332, 304, 276. Calc. for $C_8H_{10}^{98}MoO_4S_2$; (P)$^+$ 332, (P − CO)$^+$ 304, (P − 2CO)$^+$ 276.

4.13. [Mo(CO)$_4${MeS(CH$_2$)$_3$SMe}]

Yield 63% (Found: C, 31.2; H, 3.5. $C_9H_{12}MoO_4S_2$ requires C, 31.4; H, 3.5%). FAB-MS M$^+$ 346, 318. Calc. for $C_9H_{12}^{98}MoO_4S_2$; (P)$^+$ 346, (P − CO)$^+$ 318.

4.14. [Mo(CO)$_4${o-C$_6$H$_4$(SMe)$_2$}] · 1/2CH$_2$Cl$_2$

Yield 63% (Found: C, 35.6; H, 2.6. $C_{10.5}H_{11}ClMoO_4S_2$ requires C, 35.6; H, 2.6%).

4.15. [Mo(CO)$_4${MeSe(CH$_2$)$_2$SeMe}]

Yield 61% (Found: C, 22.8; H, 2.5. $C_8H_{10}MoO_4Se_2$ requires C, 22.7; H, 2.4%). FAB-MS M$^+$ 424, 398, 370. Calc. for $C_8H_{10}^{98}MoO_4^{80}Se_2$; (P)$^+$ 428, (P − CO)$^+$ 400, (P − 2CO)$^+$ 372.

4.16. [Mo(CO)$_4${MeSe(CH$_2$)$_3$SeMe}]

Yield 73% (Found: C, 24.8; H, 2.4. $C_9H_{12}MoO_4Se_2$ requires C, 24.7; H, 2.7%). FAB-MS M$^+$ 440, 410. Calc. for $C_9H_{12}^{98}MoO_4^{80}Se_2$; (P)$^+$ 442, (P − CO)$^+$ 414.

4.17. [Mo(CO)$_4${o-C$_6$H$_4$(SeMe)$_2$}]

Yield 73% (Found: C, 29.7; H, 2.1. $C_{12}H_{10}MoO_4Se_2$ requires C, 30.5; H, 2.1%).

4.18. [W(CO)$_4${MeTe(CH$_2$)$_3$TeMe}]

[W(CO)$_4$(Me$_2$N(CH$_2$)$_3$NMe$_2$)] (0.12g, 0.28 mmol) was dissolved in degassed toluene (15 cm^3) and the ligand (0.09 g, 0.28 mmol) added via a syringe. The reaction mixture was stirred at 70°C overnight and then the toluene removed in vacuo. The residue was dissolved in CHCl$_3$ (5 cm^3), filtered and cold *n*-pentane added to yield a pale yellow powder. This was filtered off, washed with *n*-pentane and vacuum dried. Yield 0.09 g 53%. (Found: C, 17.5; H, 1.9. $C_9H_{12}O_4Te_2W$ requires C, 17.3; H, 1.9%). FAB-MS M$^+$ 623. Calc. for $C_9H_{12}O_4^{130}Te_2^{184}W$; (P)$^+$ 628.

4.19. [W(CO)$_4${o-C$_6$H$_4$(TeMe)$_2$}]

Yield 71% (Found: C, 22.0; H, 1.7. $C_{12}H_{10}O_4Te_2W$ requires C, 21.9; H, 1.5%). FAB-MS M$^+$ 657. Calc. for $C_{12}H_{10}O_4^{130}Te_2^{184}W$; (P)$^+$ 662.

4.20. [W(CO)$_4${PhTe(CH$_2$)$_3$TePh}]

Yield 63% (Found: C, 29.7; H, 2.1. $C_{19}H_{16}O_4Te_2W$ requires C, 30.5; H, 2.1%). FAB-MS M$^+$ 747. Calc. for $C_{19}H_{16}O_4^{130}Te_2^{184}W$; (P)$^+$ 752.

4.21. [W(CO)$_4${MeS(CH$_2$)$_2$SMe}]

Yield 73% (Found: C, 22.8; H, 2.4. $C_8H_{10}O_4S_2W$ requires C, 23.0; H, 2.4%). FAB-MS M$^+$ 418, 390. Calc. for $C_8H_{10}O_4^{32}S_2^{184}W$; (P)$^+$ 418, (P − 2CO)$^+$ 390.

4.22. [WCO)$_4${MeS(CH$_2$)$_3$SMe}]

Yield 70% (Found: C, 24.6; H, 2.7. $C_9H_{12}O_4S_2W$ requires C, 25.0; H, 2.7%). FAB-MS M$^+$ 432, 404. Calc. for $C_9H_{12}O_4S_2^{184}W$; (P)$^+$ 432, (P − 2CO)$^+$ 404.

4.23. [W(CO)$_4${MeSe(CH$_2$)$_2$SeMe}]

Yield 60% (Found: C, 18.9; H, 2.1. $C_8H_{10}O_4Se_2W$ requires C, 18.8; H, 2.1%).

4.24. [W(CO)$_4${MeSe(CH$_2$)$_3$SeMe}]

Yield 75% (Found: C, 20.6; H, 2.4. $C_9H_{12}O_4Se_2W$ requires C, 20.5; H, 2.3%). FAB-MS M$^+$ 526, 498. Calc. for $C_9H_{12}O_4^{80}Se_2^{184}W$; (P)$^+$ 528, (P − CO)$^+$ 500.

4.25. [W(CO)$_4${o-C$_6$H$_4$(SeMe)$_2$}]

Yield 68% (Found: C, 25.6; H, 2.0. $C_{12}H_{10}O_4Se_2W$ requires C, 25.7; H, 1.8%). FAB-MS M$^+$ 560, 532, 504. Calc. for $C_{12}H_{10}O_4^{80}Se_2^{184}W$; (P)$^+$ 562, (P − CO)$^+$ 534, (P − 2CO)$^+$ 506.

4.26. Crystal structure of [Cr(CO)$_4$(MeSeCH$_2$CH$_2$SeMe)]

Details of the crystallographic data collection and refinement parameters are given in Table 5. The crystals were grown by vapour diffusion of *n*-pentane into a solution of the complex in chloroform. Data collection used a Rigaku AFC7S four-circle diffractometer

Table 5
Data collection parameters for [Cr(CO)$_4$(MeSeCH$_2$CH$_2$SeMe)]

Formula	$C_8H_{10}CrO_4Se_2$
Formula weight	380.08
Space group	$P\bar{1}$
a (Å)	8.069(5)
b (Å)	11.314(8)
c (Å)	7.909(4)
α (°)	91.41(6)
β (°)	115.74(4)
γ (°)	69.43(5)
V (Å^3)	601.8(8)
Z	2
D_{calc} (g cm^{-3})	2.097
μ(Mo–K$_\alpha$) (cm^{-1})	69.89
Ψ-scans (max./min. transmission factors)	1.000/0.507
Unique observed reflections	2125
Observed reflections with $[I_o = 2\sigma(I_o)]$	1698
No. of parameters	136
R[a]	0.038
R_w[b]	0.037

[a] $R = \Sigma(|F_o|_i - |F_c|_i)/\Sigma |F_o|_i$.

[b] $R_w = \sqrt{[\Sigma w_i(|F_o|_i - |F_c|_i)^2/\Sigma w_i|F_o|_i^2]}$.

equipped with an Oxford Systems open-flow cryostat operating at 150 K and using graphite-monochromated Mo–Kα X-radiation ($\lambda = 0.71073$ Å). No significant crystal decay or movement was observed. The structure was solved by direct methods [24] and developed by iterative cycles of full-matrix least-squares refinement and difference Fourier syntheses [25]. All non-H atoms were refined anisotropically while H-atoms were placed in fixed, calculated positions with d(C–H) = 0.96 Å. The weighting scheme $w^{-1} = \sigma^2(F)$ gave satisfactory agreement analyses. Selected bond lengths and angles are given in Table 4.

5. Supplementary material

Crystallographic data for H-atom coordinates, anisotropic thermal parameters and full listings of bond lengths and angles for the structure have been deposited with the Cambridge Crystallographic Data Centre. Copies of this information may be obtained free of charge from The Director, CCDC, 12 Union Road, Cambridge, CB2 1EZ, UK (fax: +44-1223-336-033; e-mail: deposit@ccdc.ac.uk or www: http://www.ccdc.cam.ac.uk).

Acknowledgements

The authors thank EPSRC for support.

References

[1] E.W. Abel, F.G.A. Stone, G. Wilkinson (eds.), Comprehensive Organometallic Chemistry I and II, Pergammon, Oxford, 1982, 1995.

[2] E.G. Hope, W. Levason, Coord. Chem. Rev. 122 (1993) 103.

[3] (a) T. Kemmitt, W. Levason, M. Webster, Inorg. Chem. 28 (1989) 692. (b) T. Kemmitt, W. Levason, Inorg. Chem. 29 (1990) 731.

[4] (a) R.A. Cipriano, L.R. Hanton, W. Levason, D. Pletcher, N.A. Powell, M. Webster, J. Chem. Soc. Dalton Trans. (1988) 2483. (b) J.L. Brown, T. Kemmitt, W. Levason, J. Chem. Soc. Dalton Trans. (1990) 1513.

[5] (a) J.R. Black, N.R. Champness, W. Levason, G. Reid, J. Chem. Soc. Dalton Trans. (1995) 3439. (b) J.R. Black, N.R. Champness, W. Levason, G. Reid, Inorg. Chem. 35 (1996) 1820.

[6] E.W. Abel, K.G. Orrell, S.P. Scanlan, D. Stevenson, T. Kemmitt, W. Levason, J. Chem. Soc. Dalton Trans. (1991) 591.

[7] W. Levason, S.D. Orchard, G. Reid, Organometallics (1999) in press.

[8] (a) R. Donaldson, G. Hunter, R.C. Massey, J. Chem. Soc. Dalton Trans. (1974) 288. (b) G. Hunter, R.C. Massey, J. Chem. Soc. Dalton Trans. (1975) 209; (1976) 2007.

[9] E.W. Ainscough, E.J. Birch, A.M. Brodie, Inorg. Chim. Acta 20 (1976) 187.

[10] E.N. Baker, N.G. Larsen, J. Chem. Soc. Dalton Trans. (1976) 1769.

[11] H.C.E. Mannerskantz, G. Wilkinson, J. Chem. Soc. (1962) 4454.

[12] R. Ros, M. Vitali, R. Graziani, Gazz. Chim. Ital. 100 (1970) 407.

[13] E.W. Abel, G.V. Hutson, J. Inorg. Nucl. Chem. 31 (1969) 3333.

[14] E.W. Abel, D.E. Budgen, I. Moss, K.G. Orrell, V. Sik, J. Organomet. Chem. 362 (1989) 105.

[15] E.W. Abel, I. Moss, K.G. Orrell, V. Sik, J. Organomet. Chem. 326 (1987) 187.

[16] E.W. Abel, M.A.Z. Chowdhury, K.G. Orrell, V. Sik, J. Organomet. Chem. 262 (1984) 293.

[17] (a) D.E. Halverson, G.M. Reisner, G.R. Dobson, I. Bernal, T.L. Mulcahy, Inorg. Chem. 21 (1982) 4285. (b) G.M. Reisner, I. Bernal, G.R. Dobson, J. Organomet. Chem. 157 (1978) 23.

[18] E.W. Abel, S.K. Bhargava, K.G. Orrell, Prog. Inorg. Chem. 32 (1984) 1.

[19] H. Schumann, A.A. Arif, A.L Rheingold, C. Janiak, R. Hoffmann, N. Kuhn, Inorg. Chem. 30 (1991) 1618.

[20] N.P. Luthra, J.D. Odom, in: S. Patai, Z. Rappoport (eds.), The Chemistry of Organic Selenium and Tellurium Compounds, Wiley, New York, 1986, Chapter 6.

[21] J.J. Eisch, R.B. King, Organomet. Syn. 1 (1965) 122.

[22] G.R. Dobson, G.C. Faber, Inorg. Chim. Acta. 4 (1987) 87.

[23] (a) E.G. Hope, T. Kemmitt, W. Levason, Organometallics 7 (1988) 78. (b) T. Kemmitt, W. Levason, Organometallics 8 (1989) 1303.

[24] G.M. Sheldrick, SHELXS86, Program for crystal structure solution, Acta Crystallogr. Sect. A 46 (1990) 467.

[25] TeXsan: Crystal Structure Analysis Package, Molecular Structure Corporation, Texas, 1995.